Available online at www.sciencedirect.com
SCIENCE DIRECT
Journal of Crystal Growth 259 (2003) 115–120
JOURNAL OF CRYSTAL GROWTH
www.elsevier.com/locate/jcrysgro

Growth of high-quality β_{II}-Li_3VO_4 single crystals by the Czochralski method

Dong Jin Kim[a], Yoon-Hwae Hwang[b,*], Hyung Kook Kim[b], Jung Nam Kim[b], Yoshinobu Kasuga[c], Ken-ichi Ohshima[c]

[a] ECC, Dong-Eui University, Busan 614-714, South Korea
[b] RCDAMP and Department of Physics, Pusan National University, San 30 Jangjeon-Dong, Keumjong, Busan 609-735, South Korea
[c] Institute of Materials Science, University of Tsukuba, Tsukuba 305-8573, Japan

Received 25 March 2003; accepted 19 July 2003
Communicated by T. Hibiya

Abstract

We have successfully grown colorless and crack-free β_{II}-Li_3VO_4 single crystals by the Czochralski method using a self-flux. To improve the quantity of crystals, we installed a heat reservoir in the growing furnace, used the melt composition as Li_2CO_3:V_2O_5 = 58:42 (Li/58) to avoid the unnecessary phase transition and set the growth temperature below 700°C to avoid the cracking. The physical properties of the crystals were studied by the powder X-ray diffraction, impedance/gain phase, differential thermal analysis (DTA), and UV–VIS transmittance spectroscopy measurements. We found that the physical properties of Li/58 crystals were almost identical to those of Li/70 crystals except the UV–VIS transmittance data.

PACS: 61.10.Nz; 64.90.+b; 65.70.+y; 81.10.−h

Keywords: A1. Differential thermal analysis; A1. X-ray diffraction; A2. Czochralski method; B1. β_{II}-Li_3VO_4 single crystal; B1. Lithium vanadate

1. Introduction

Low-temperature phase of lithium vanadate, β_{II}-Li_3VO_4, have attractive properties for optic materials and ionic conduction materials. In previous studies of lithium vanadate, Sakata et al. [1,2] found that β_{II}-Li_3VO_4 have second harmonic generation(SHG) activity, and Gaur et al. [3] extensively studied the electrical conductivity, σ, of Li_3VO_4 solidified melt. Three methods have been carried out to obtain high-quality Li_3VO_4 crystals such as floating-zone method, Czochralski method and heater-in-zone zone-melting method. Sakata et al. [4] and Itoyama et al. [5] obtained a crack free, and transparent β_{II}-Li_3VO_4 crystals by the floating-zone method. Kim et al. [6] and Higuchi et al. [7] recently grew crack-free, and transparent β_{II}-Li_3VO_4 crystals by the Czochralski method and heater-in-zone zone-melting method,

*Corresponding author.
E-mail address: yhwang@pusan.ac.kr (Y.-H. Hwang).

0022-0248/$ - see front matter © 2003 Elsevier B.V. All rights reserved.
doi:10.1016/S0022-0248(03)01594-X

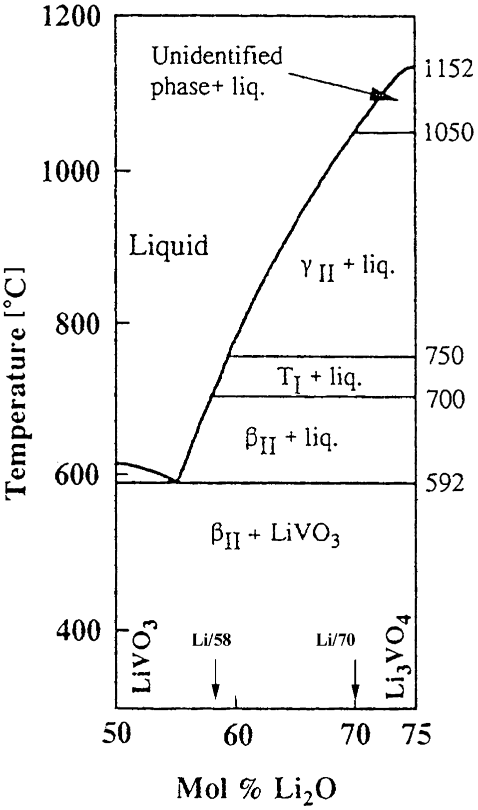

Fig. 1. Phase diagram of Li_2CO_3–V_2O_5 system [4]. Two arrows in this figure indicate melt compositions used in this study.

respectively. As shown in Fig. 1, phase diagrams of the Li_2O–V_2O_5 system indicate that Li_3VO_4 melts congruently, however, it undergoes phase transitions between the melting point and room temperature. Accordingly, the melt-grown crystals contain many micro-cracks because of the phase transitions [4].

In this study, we carefully considered the growth conditions to obtain a high-quality β_{II}-Li_3VO_4 single crystals so that we have successfully grown colorless and crack-free β_{II}-Li_3VO_4 single crystals by the Czochralski method using a self-flux. We installed a heat reservoir in the growing furnace to improve the temperature gradient of growing furnace, used the melt composition as Li_2CO_3:V_2O_5 = 58:42 (Li/58) to avoid the unnecessary phase transition, and set the growth temperature below 700°C to reduce the number of cracks. The physical properties of Li/58 crystals were almost identical to those of Li/70 crystals except the UV–VIS transmittance data.

2. Experiment

The raw materials for β_{II}-Li_3VO_4 crystal growth were Li_2CO_3 (ALDRICH, 99.9%) and V_2O_5 (ALDRICH, 99.9%). Fig. 1 shows a relation between Li_2O molar ratios and growth temperatures. In our laboratory, we grew β_{II}-Li_3VO_4 crystals using two melt compositions which were Li_2CO_3:V_2O_5 = 70:30 (Li/70) and Li_2CO_3:V_2O_5 = 58:42 (Li/58). A more detailed information about vanadium-rich composition Li/70 crystal growth is available in our previous study [6]. The growth conditions of Li/58 crystals were very similar to those of Li/70 crystals. When we grew Li/58 crystals, however, we carefully set up the growth conditions to obtain a high-quality β_{II}-Li_3VO_4 single crystals. We installed a heat reservoir in the growing furnace to improve the temperature gradient of growing furnace and set the growth temperature below 700°C to reduce the number of the cracks.

The structure of β_{II}-Li_3VO_4 crystal was verified by the X-ray diffraction (XRD, Rigaku GDX-1193A) for Cu Kα radiation and a polarizing optical microscope. Also the physical properties of the grown β_{II}-Li_3VO_4 single crystals were characterized by impedance/gain phase analyzer (HP4194A), differential thermal analysis (DTA, MAC Science, WS002 II), and high-temperature X-ray diffraction (Philips PW3050) experiments. The phase transition properties of crystals were investigated by impedance, DTA, and high-temperature XRD measurements. The temperature-dependent dielectric constants were measured by using an impedance analyzer at the frequency of 500 Hz. The temperature range used in this study were from room temperature to 800°C. The DTA data were measured with a heating rate of 5°C/min. The high-temperature XRD experiments were carried out by employing the high-temperature diffractometer. The XRD patterns were recorded at different temperatures ranging from room temperature to 900°C, in the 2θ range of 10°–90°. The cell constants at different temperatures were obtained from the d-values of reflections and were refined by the least-squares fit method. The transmittance measurements were also performed by using UV–VIS spectrometer (Cary5, Varian, Australia) in the wavelength range of 200–3600 nm.

3. Results and discussion

The most serious problem in the growth of β_{II}-Li_3VO_4 single crystals is the formation of micro-cracks [4]. A phase diagram of Li_2O–V_2O_5 system in Fig. 1 indicates that Li_3VO_4 melts congruently [8,9], but it undergoes three phase transitions between the melting point and room temperature. Accordingly, the melt-grown β_{II}-Li_3VO_4 crystals contain many micro-cracks because of those phase transitions. Sakata et al. [4] introduced the travelling solvent floating zone method using an image furnace to grow high-quality β_{II}-Li_3VO_4 crystals. However, the grown crystals had many macroscopic defects such as micro-cracks and inclusions. We have tried to obtain a crack-free crystals by the Czochralski method for many years. As predicted in the phase diagram, we found that phase transitions during the cooling caused micro-cracks when a crystal was grown from a stoichiometric melt, as pointed out by Sakata et al. [4]. When we used a vanadium-rich composition Li_2CO_3:V_2O_5 = 70:30 (Li/70) in molar ratio, we could obtain relatively crack-free transparent crystals. But the grown crystals still show a weak orange color [6].

Based on findings in our previous study, we carefully set up the growth conditions to obtain a high-quality β_{II}-Li_3VO_4 single crystals. We installed a heat reservoir in the growing furnace. The installation of heat reservoir could lessen thermal stress in growing furnace [6,10]. We used the melt compositions as Li_2CO_3:V_2O_5 = 58:42 (Li/58) to avoid unnecessary phase transitions. However, the vanadium-rich composition might have increased the viscosity of the melt and it could make difficult to get β_{II}-Li_3VO_4 single crystals. The other problem to be settled was the bubble accumulation in as-grown crystals: i.e., the single crystal ended up having many micro-pores inside [5]. Therefore, the avoidance of the bubble accumulation was essential in growing a large single crystal. To resolve above problems, we used a low growth rate less than 0.2 mm/h and a rotation rate around 23 rpm. Also, the growing temperature was set below 700°C to prevent the crystals from cracking [7]. As a result of improvements in the crystal growth technique, we could grow a large colorless crystal (6 mm diameter, 20 mm length) with no cracks.

Figs. 2(a) and (b) show the photograph of β_{II}-Li_3VO_4 single crystals grown along the [1 0 0] direction with Li/70 and Li/58 melt compositions, respectively. β_{II}-Li_3VO_4 single crystal of Li/70 melt composition has an orange color and a few cracks. On the other hand, as-grown crystal with Li/58 melt composition is transparent, color-free and has no cracks. We also tested the quality of crystals by using polarizing micrographs of a cross section of the [1 0 0] direction. The results are shown in Figs. 3(a) and (b) for crystals with Li/70 and Li/58 melt composition, respectively. As-grown crystal of Li/70 melt composition shows low-angle subgrain boundaries and a small number of impurities. On the other hand, Li/58

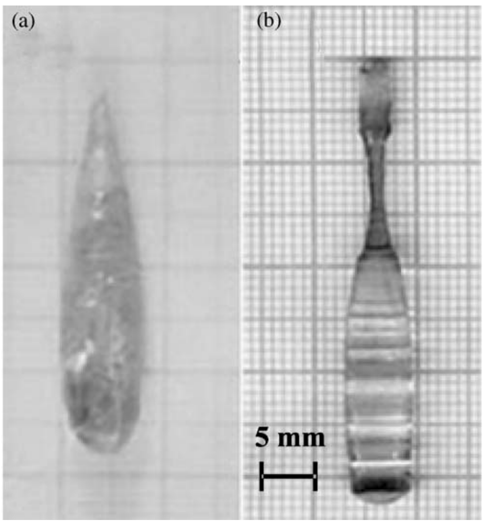

Fig. 2. Li_3VO_4 single crystals grown by the Czochralski method using the self-flux for (a) Li/70 and (b) Li/58 melt composition.

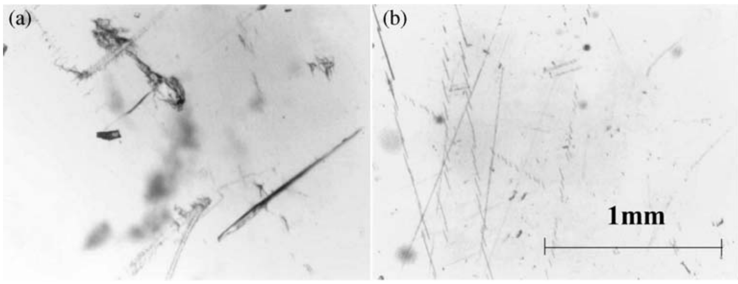

Fig. 3. Polarizing micrographs of cross section of β_{II}-Li_3VO_4 crystals grown along the [1 0 0] direction for (a) Li/70 and (b) Li/58 melt composition.

shows no low-angle grain boundary. These results indicate that there is a lower possibility of grain-boundary-free β_{II}-Li_3VO_4 crystals by Li/58 melt composition. Therefore, crystal growing with Li/58 melt composition is necessary to obtain high-quality β_{II}-Li_3VO_4 single crystal [7]. Previously Higuchi et al. also succeeded in growing grain-boundary-free β_{II}-Li_3VO_4 crystals by growing them along the [0 0 1] direction. We tested the physical properties of two Li_3VO_4 single crystals by using high-temperature powder X-ray diffraction, impedance/gain phase, differential thermal analysis (DTA), and UV–VIS transmittance spectroscopy experiments.

We first tested the structure of two crystals at room temperature. The X-ray diffraction patterns of β_{II}-Li_3VO_4 with Li/70 and Li/58 compositions were identical and corresponded to the β_{II} phase. The cell parameters of the β_{II}-Li_3VO_4 crystals were determined by fitting the diffraction data with all possible cell configurations. From the best-fitting results, we found that the unit cell structure was orthorhombic with $a = 5.4432$, $b = 6.3156$, $c = 4.9436$ Å for Li/70 composition and $a = 5.4422$, $b = 6.3301$, $c = 4.9445$ Å for Li/58 composition. Within an uncertainty in the data analysis, lattice parameters of Li/70 and Li/58 crystals were consistent with each other and agreed well with the results of other studies [11,12]. The values of the lattice parameters correspond to the β_{II} phase of Li_3VO_4 [11].

Next, we characterized phase transition properties of two β_{II}-Li_3VO_4 crystals. To this end, we performed dielectric, DTA and high-temperature X-ray diffraction measurements. Fig. 4 shows the temperature dependent of real part of dielectric constant along a-axis at frequency of 500 Hz. The inset of Fig. 4 shows the dielectric data in the extended temperature range down to room temperature. In this figure, we can observe dielectric anomalies in both crystals. Li/70 crystal showed dielectric anomalies at temperatures around 350°C, 710°C, and 760°C. On the other hand, Li/58 crystal showed dielectric anomalies at temperatures around 400°C, 730°C, and 780°C. It seemed that Li/70 crystal showed dielectric anomalies at lower temperatures compared to those of Li/58 crystals. In our previous study, we identified anomalies at temperatures higher than 700°C were related to structural transitions [6]. The DTA data were measured with a heating rate of 5°C/min and the results are shown in Fig. 5. Both crystals showed two endothermic peaks around 720°C and 770°C and the results were consistent with other studies [9]. The peak positions of Li/70 crystal and Li/58 crystal were 720°C, 773°C and 715°C, 768°C, respectively. It seemed that Li/70 crystals showed higher transition temperatures compared to those of Li/58 crystals. We also studied the change of the crystal lattice parameters at different temperatures. The lattice constants of Li/70 and Li/58 crystals were calculated from the temperature dependent X-ray diffraction data and the results are shown in Fig. 6. We can observe that the temperature dependent lattice parameters of Li/70 and Li/58 crystals were almost the same. The lattice constants exhibits anomalies at temperature around 710°C, and 790°C.

In three different experiments, we could not find any consistent trend of transition temperatures for Li/58 and Li/70 crystals. The trend in DTA

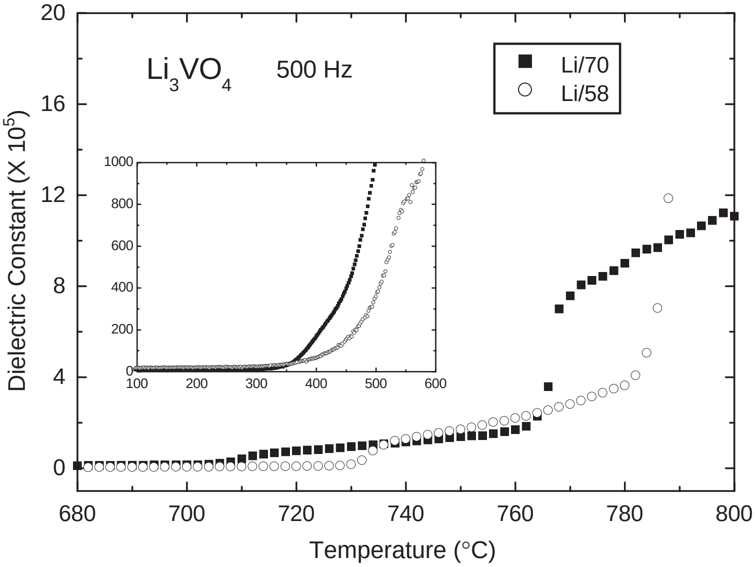

Fig. 4. The temperature dependence of real part of dielectric constant along *a*-axis for β_{II}-Li_3VO_4 single crystal at 500 Hz. The inset is the dielectric constant in the temperature range from 100°C–600°C. Solid squares and open circles correspond to crystals grown from Li/70 and Li/58 melt compositions, respectively.

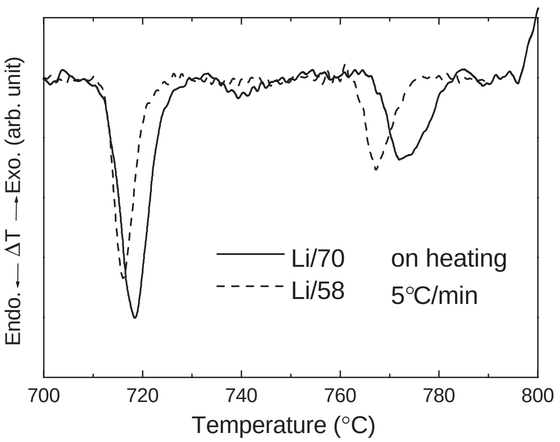

Fig. 5. DTA data of β_{II}-Li_3VO_4 single crystals in the heating process. In this data, the heating rate was 5°C/min. The solid line and dashed line correspond to crystals grown from Li/70 and Li/58 melt compositions, respectively.

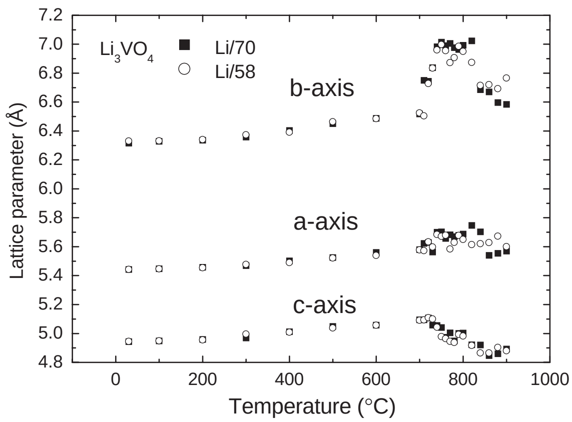

Fig. 6. Temperature dependent lattice parameters calculated from high-temperature X-ray diffraction data. Solid squares and open circles correspond to crystals grown from Li/70 and Li/58 melt compositions, respectively.

measurements was opposite to that in dielectric measurements and XRD measurements showed almost same transition temperatures for both crystals. Therefore, at this stage, we just speculate that the different transition temperatures observed in different experiments may originate from experimental uncertainties. We may ask why there was no structural change in X-ray data at temperature around 400°C where we observed dielectric anomaly. In our previous study, we found that this anomaly is related to the dissociation of Li–O bond, not related to a structural

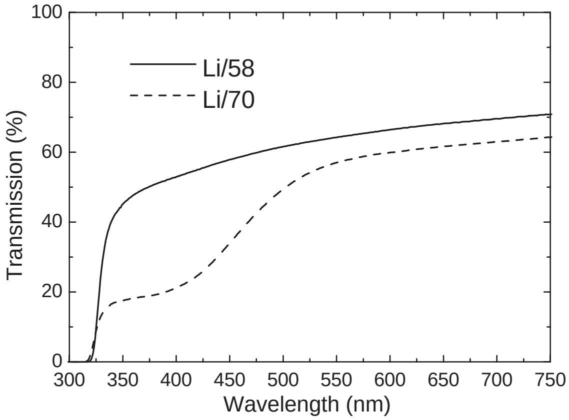

Fig. 7. UV–VIS transmittance spectra of β_{II}-Li_3VO_4 single crystals of about 0.7 mm thickness for both Li/70 and Li/58 crystals. The measurements were done at room temperature. The solid line and the dashed line correspond to crystals grown from Li/70 and Li/58 melt compositions, respectively.

change [13]. Therefore, dielectric anomalies around 400°C might originate from not only an experimental uncertainty but also from different Li contents in the samples. A more detailed study is in progress and the results will be published in the future.

Fig. 7 shows the UV–VIS transmittance of the as-grown β_{II}-Li_3VO_4 single crystals made from Li/70 and Li/58 melt compositions. As we already observed in Fig. 2, Li/70 crystals had the weak orange color, but Li/58 crystals were transparent. Therefore, the transmittance data from two crystals were different. In Li/70 crystals, there existed an optical absorption band at 350–500 nm due to the orange color. Besides this difference, both samples showed the same absorption edge around 320 nm.

4. Conclusion

We have successfully grown colorless and crack-free β_{II}-Li_3VO_4 single crystals by the Czochralski method using a self-flux. The significant improvements in the crystal quality can be achieved by installation of heat reservoir to the growing furnace, using the melt compositions as Li_2CO_3:V_2O_5 = 58:42 (Li/58) and setting the growth temperature below 700°C. The temperature of the molten zone was precisely controlled by a low growth rate of less 0.2 mm/h and a rotation rate of 20–30 rpm.

The structure of as-grown crystal was identified by X-ray diffraction and confirmed as β_{II} phase. The phase transition properties of both Li/70 and Li/58 crystals were characterized by three different experiments, dielectric, DTA and high-temperature XRD measurements. The results were consistent with each other within experimental uncertainties and showed anomalies at temperatures around 720°C and 780°C. In UV–VIS transmittance measurement, β_{II}-Li_3VO_4 crystal has almost the same absorption edge, approximately 320 nm. But β_{II}-Li_3VO_4 single crystals with Li/70 melt composition had the optical absorption band at 350–500 nm due to the orange color in the sample.

Acknowledgements

This work was supported by Korea Research Foundation Grant (KRF-2000-015-DP0105).

References

[1] S. Sakata, I. Fujii, Jpn. J. Appl. Phys. 30 (1991) L1489.
[2] S. Sakata, N. Ueda, I. Fujii, H. Kawazoe, J. Non-Cryst. Solids 178 (1994) 98.
[3] K. Gaur, A.J. Pathak, H.B. Lal, J. Mater. Sci. 23 (1988) 4257.
[4] S. Sakata, W. Itoyama, I. Fujii, K. Iishi, J. Crystal Growth 135 (1994) 555.
[5] W. Itoyama, K. Iishi, S. Sakata, J. Crystal Growth 158 (1996) 534.
[6] D.J. Kim, J.S. Kim, J.N. Kim, M.S. Jang, J. Crystal Growth 217 (2000) 383.
[7] M. Higuchi, Y. Chuman, T. Kitagawa, K. Kodaira, J. Crystal Growth 216 (2000) 322.
[8] A. Reisman, J. Mineo, J. Phys. Chem. 66 (1962) 1181.
[9] A.R. West, P. Glasser, J. Solid State Chem 4 (1972) 20.
[10] J.C. Rojo, E. Dieguez, J.J. Derby, J. Crystal Growth 200 (2000) 329.
[11] S.B. Pfoertsch, Z. Smith, Penn State University, University Park, PA, USA, ICDD Grant-in-Aid, 1987.
[12] R.D. Shannon, C. Calvo, J. Solid State Chem. 6 (1973) 538.
[13] D.J. Kim, B.E. Jun, C.-S. Kim, H.K. Kim, J.N. Kim, Y.-H. Hwang, J. Appl. Phys. 93 (3) (2003) 1697.